

Rare events and the convergence of exponentially averaged work values

Christopher Jarzynski¹

¹*Theoretical Division, T-13, MS B213, Los Alamos National Laboratory, Los Alamos, New Mexico 87545*
 chrisj@lanl.gov

Equilibrium free energy differences are given by exponential averages of nonequilibrium work values; such averages, however, often converge poorly, as they are dominated by rare realizations. I show that there is a simple and intuitively appealing description of these rare but dominant realizations. This description is expressed as a duality between “forward” and “reverse” processes, and provides both heuristic insights and quantitative estimates regarding the number of realizations needed for convergence of the exponential average. Analogous results apply to the equilibrium perturbation method of estimating free energy differences. The pedagogical example of a piston and gas [R.C. Lua and A.Y. Grosberg, *J. Phys. Chem. B* **109**, 6805 (2005)] is used to illustrate the general discussion.

The nonequilibrium work theorem,

$$\langle e^{-\beta W} \rangle = e^{-\beta \Delta F}, \quad (1)$$

relates the work performed on a system during a nonequilibrium process, to the free energy difference between two equilibrium states of that system. The angular brackets denote an average over an ensemble of realizations (repetitions) of a thermodynamic process, during which a system evolves in time as a control parameter λ is varied from an initial value A to a final value B . W is the external work performed on the system during one realization; $\Delta F = F_B - F_A$ is the free energy difference between two equilibrium states of the system, corresponding to $\lambda = A$ and B ; and β is the inverse temperature of a heat reservoir with which the system is equilibrated prior to the start of each realization of the process. A sample of derivations of Eq. 1 can be found in Refs. [1, 2, 3, 4, 5, 6, 7, 8, 9, 10]; pedagogical and review treatments are given in Refs. [11, 12, 13, 14, 15, 16]; for experimental tests of this and closely related results, see Refs. [17, 18, 19, 20]; finally, Refs. [21, 22, 23, 24, 25] discuss quantal versions of the theorem.

In principle, Eq.1 implies that ΔF can be estimated using nonequilibrium experiments or numerical simulations. If we repeat the thermodynamic process N times, and observe work values W_1, W_2, \dots, W_N , then

$$\Delta F \approx -\beta^{-1} \ln \left[\frac{1}{N} \sum_{n=1}^N e^{-\beta W_n} \right], \quad (2)$$

where the approximation becomes an equality in the limit of infinitely many realizations, $N \rightarrow \infty$. In practice, the average of $e^{-\beta W}$ is often dominated by very rare realizations, leading to poor convergence with N . The aim of this paper is develop an understanding of these rare but important realizations. I will argue that there is a simple description of these dominant realizations, which leads to both quantitative estimates and useful heuristic insights regarding the number of realizations needed for convergence of the average of $e^{-\beta W}$.

The organization of this paper is as follows. In Section I the central result is summarized, then illustrated using a simple example. Section II contains a derivation of this result. Section III discusses the number of realizations needed for convergence of the exponential average. Section IV focuses on the free energy perturbation method (a limiting case of Eq.1), and Section V concludes with a brief discussion.

I. SUMMARY AND ILLUSTRATION OF CENTRAL RESULT

The average in Eq.1 can be written as

$$\langle e^{-\beta W} \rangle = \int dW \rho(W) e^{-\beta W} \equiv \int dW g(W), \quad (3)$$

where $\rho(W)$ is the ensemble distribution of work values. Fig.1 shows a schematic plot of this distribution, and of the integrand in Eq.3, $g(W) = \rho(W) e^{-\beta W}$. While ρ is peaked near the mean of the distribution,

$$\bar{W} = \int dW \rho(W) W, \quad (4)$$

g is peaked around a lower value, W^\dagger , as the factor $e^{-\beta W}$ has the effect of strongly weighting those work values that are in the far left tail of ρ . Explicitly,

$$W^\dagger = c^{-1} \int dW g(W) W, \quad (5)$$

where $c = \int dW g(W)$. As pointed out by Ritort in the context of a “trajectory thermodynamics” formalism [26], the average of $e^{-\beta W}$ is dominated by the region near the peak of the integrand of Eq.3, i.e. near W^\dagger . I will use the term *typical* to refer to those realizations whose work values are near the peak of ρ , and *dominant* to refer to those for which the work is near the peak of g . Typical realizations are the ones that we ordinarily observe when carrying out the process, while dominant realizations are those rare realizations that contribute the greatest share to the average of $e^{-\beta W}$.

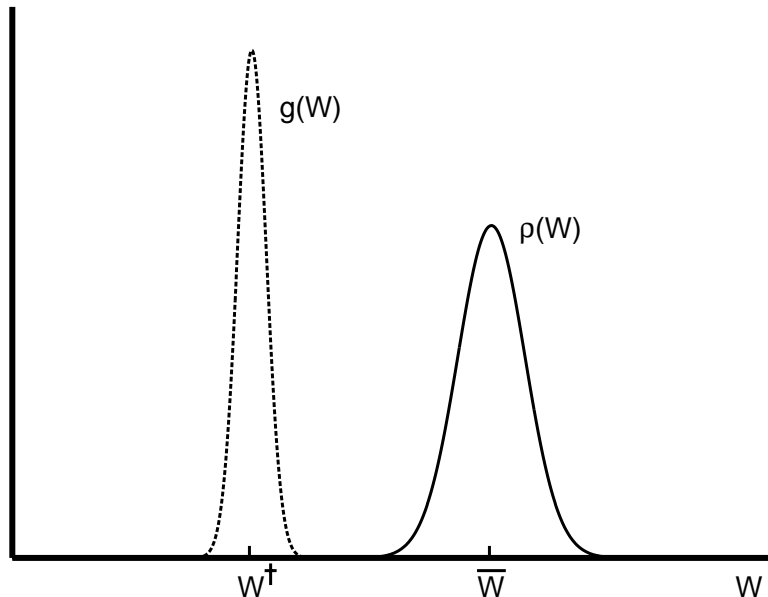


FIG. 1: During most realizations of the process, we observe work values near the peak of $\rho(W)$. However, the average of $e^{-\beta W}$ is dominated by realizations for which the work is observed to be in the region around the peak of $g(W) = \rho(W)e^{-\beta W}$.

For the process discussed in the previous paragraph, the work parameter λ is varied from A to B . Following Crooks [2], let us also consider a process during which λ is manipulated from B to A , and let us use the terms *forward* (F) and *reverse* (R) to distinguish between the two processes. Specifically, if λ_t^F denotes the schedule for varying the work parameter during the forward process, from $\lambda_0^F = A$ to $\lambda_\tau^F = B$, then the reverse process is defined by the schedule

$$\lambda_t^R = \lambda_{\tau-t}^F, \quad (6)$$

where τ is the duration of either process.

Note that the nonequilibrium work theorem applies to both processes:

$$\langle e^{-\beta W} \rangle_F = e^{-\beta \Delta F} \quad , \quad \langle e^{-\beta W} \rangle_R = e^{+\beta \Delta F}, \quad (7)$$

where $\langle \dots \rangle_{F/R}$ denotes an average over realizations of the forward/reverse process; and by convention $\Delta F \equiv F_B - F_A$ in both equations. As with the forward process, it is useful to distinguish between *typical* realizations of the reverse process, and the *dominant* realizations that contribute the most to $\langle e^{-\beta W} \rangle_R$.

Throughout this paper, the evolution of the system is modeled as a Hamiltonian trajectory in phase space, where the Hamiltonian is made time-dependent by externally varying the work parameter. (See Section V for a brief discussion of other, e.g. stochastic, models.) In the absence of magnetic fields¹ – more precisely, under the assumption of

¹ When magnetic fields are present, the conjugate pairing of trajectories occurs if the reverse process is defined not only by Eq. 6, but also

time-reversal invariance, Eq.13 – forward and reverse realizations come in *conjugate pairs* related by time-reversal, as illustrated in Fig.2: if a phase space trajectory Γ_t^F represents a possible realization of the forward process (a solution of Hamilton's equations when λ is varied from A to B), then its conjugate twin,

$$\Gamma_t^R = \Gamma_{\tau-t}^{F*}, \quad (8)$$

represents a possible realization of the reverse process. The asterisk denotes a reversal of momenta: $(\mathbf{q}, \mathbf{p})^* = (\mathbf{q}, -\mathbf{p})$. The trajectory Γ_t^R depicts the sequence of events that we would observe, if we were to film the forward realization Γ_t^F and then run the movie backward.

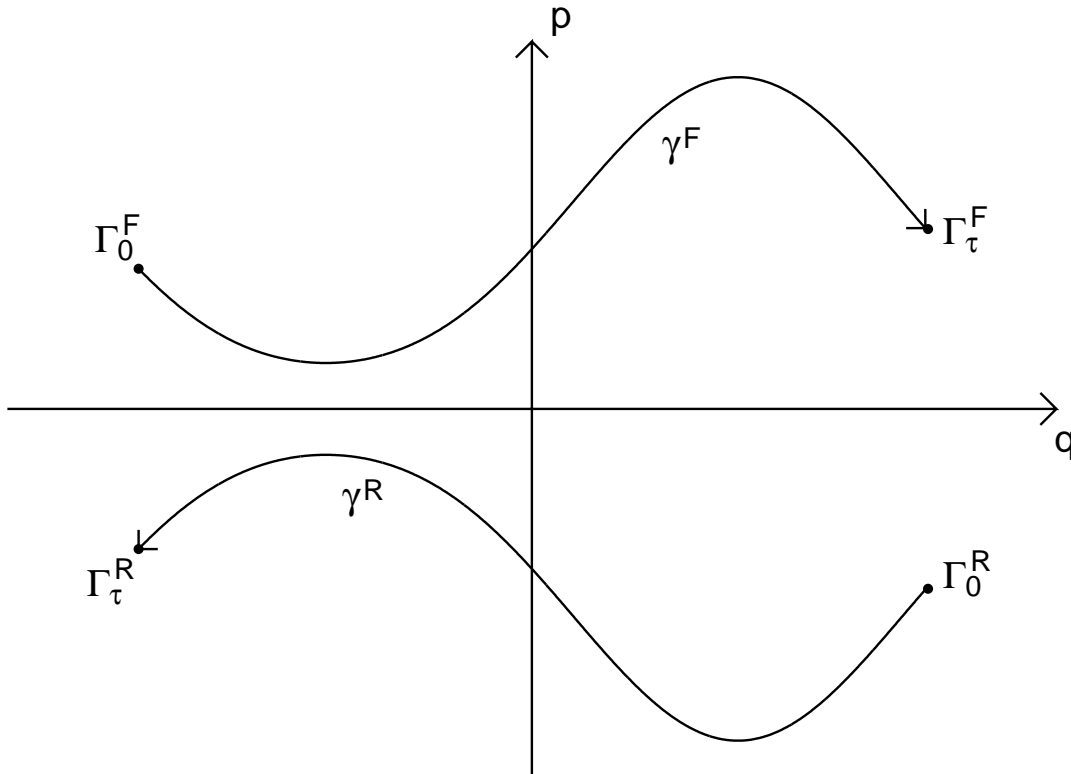


FIG. 2: A conjugate pair of trajectories. The horizontal axis (\mathbf{q}) represents the complete set of configurational coordinates (e.g. particle positions), while the vertical axis (\mathbf{p}) represents the set of associated momenta. Γ denotes a point in this many-dimensional phase space; and $\Gamma_t^{F/R}$ denotes a realization of the forward / reverse process, with time running from $t = 0$ to $t = \tau$. The two trajectories are related by time-reversal: $\Gamma_t^R = \Gamma_{\tau-t}^{F*}$, where $(\mathbf{q}, \mathbf{p})^* \equiv (\mathbf{q}, -\mathbf{p})$. In the notation of Section II, the upper curve is the trajectory γ^F , the lower curve is the trajectory γ^R .

The central result of this paper, Eq. 27 below, states that the *dominant* realizations of the forward process are the conjugate twins of *typical* realizations of the reverse process, and vice versa. Thus, the trajectories that contribute the most to $\langle e^{-\beta W} \rangle_F$, are those during which the behavior of the system appears *as though we had filmed a typical realization of the reverse process, and then run the movie backward*. The existence of such a duality was anticipated by Ritort, who observed that for large systems the work performed during a dominant realization of one process is (minus) the work performed during a typical realization of the conjugate process; see comments following Eq. 58 of Ref. [26].

As an illustration of this result, consider an ideal gas of (mutually non-interacting) point particles inside a box closed off at one end by a piston, and imagine that we act on the gas by pulling the piston outward. In the context of Eq.1, this system has recently been studied by several groups [27, 28, 29, 30]. Of particular relevance to the present paper is the analysis of Lua and Grosberg [27], who showed by explicit calculation that, in the fast piston limit,

by a change in the signs of these fields [3]. The central result of this paper then remains valid. For simplicity of presentation, however, I will restrict myself to the time-reversal-invariant situation, Eq. 13.

the dominant realizations are characterized by particles with initial velocities sampled from deep within the tail of a Maxwellian distribution; and for the reverse process, when the piston is pushed into the gas, the dominant realizations are those for which there are no particle-piston collisions [29]. These conclusions are consistent with the discussion below.

Let $n_p \gg 1$ be the total number of particles, each of mass m . Imagine that we begin with the piston at a location A , corresponding to a box of length L , and we prepare the gas in canonical equilibrium at temperature T , i.e. with particle velocities sampled independently from a Maxwellian distribution. Now we rapidly pull the piston outward, from A to B , over a time τ and at constant speed $u = L/\tau$, thus increasing the length of the box from L to $2L$ (Fig.3a). Since the volume of the box is doubled, the free energy difference between the equilibrium states corresponding to the piston locations A and B is

$$\Delta F = -n_p \beta^{-1} \ln 2. \quad (9)$$

During a realization of this process, whenever a particle collides with the moving piston, the particle suffers a change of kinetic energy, $\delta K = -2mu(v_x - u) < 0$, where v_x is the component of the particle's velocity parallel to the motion of the piston, prior to the collision. The total work W is the sum of such contributions.

If the process described above is the *forward* process, then the *reverse* process involves pushing the piston into the gas at speed u , from B to A (Fig.4a), starting from an initial state of thermal equilibrium. Each particle-piston collision now produces a change $\delta K = 2mu(v_x + u) > 0$ in the particle's kinetic energy. In the context of the piston and gas example, I will use the terms *expansion* and *compression* to denote the forward and reverse processes, respectively.

Now suppose the piston speed is much greater than the thermal particle speed:

$$u \gg v_{\text{th}} = \sqrt{3/m\beta}. \quad (10)$$

In this case, the particle density profile typically changes very little during expansion (Fig.3a): most particles remain in the left half of the box, and few if any collide with the piston, consequently

$$W^F \approx 0. \quad (11)$$

(The superscript indicates the forward process, i.e. expansion.)

During the compression process (Fig.4a), the piston typically collides with about half of the gas particles – roughly speaking, those initially located in right half of the box. This generates a shock wave of particles streaming leftward at approximately twice the piston speed. At time τ the front of this wave reaches the wall at $x = 0$, just as the piston arrives at A . Thus at the end of such a realization, half the particles (those untouched by the piston) are characterized by the original Maxwellian velocity distribution, while the other half have velocities with $v_x \approx -2u$. For such a realization,

$$W^R \approx \frac{n_p}{2} \cdot 2mu^2 = n_p mu^2. \quad (12)$$

If Fig. 4a illustrates the trajectory just described, then Fig.4b illustrates its conjugate twin. Here the piston begins at A , with half the particles streaming rightward at $v_x \approx +2u$. As the piston moves from A to B at speed u , each of these very fast particles collides once with the piston, losing most of its kinetic energy. At the moment the piston reaches B , the container is uniformly filled with a gas characterized by a Maxwellian velocity distribution at temperature T . Needless to say, this “anti-shock” wave represents an exotic sequence of events! When $n_p \gg 1$ and $u \gg v_{\text{th}}$, the probability of sampling an initial microstate for which half the particles have $v_x \approx +2u$ is fantastically small. However, according to the central result of this paper, rare realizations of this sort are precisely the dominant ones that contribute most to $\langle e^{-\beta W} \rangle_F$.

Similarly, the dominant realizations of the compression process are the conjugate twins of typical realizations of the expansion process. Thus to achieve convergence of $\langle e^{-\beta W} \rangle_R$, we must observe realizations during which the bulk of the gas happens to be localized in the left half of the box at $t = 0$. Then, as the piston moves rapidly from B to A , it sweeps through a largely empty region, as in Fig.3b. Again, this represents an unusual scenario: it is unlikely that the randomly sampled initial conditions are such that virtually all the particles are found in the left half of the box.

To summarize, while a typical realization of the expansion process is characterized by no piston-particle collisions, and a typical realization of the compression process is characterized by $\sim n_p/2$ collisions (Figs. 3a, 4a), for *dominant* realizations it is the other way around (Figs. 4b, 3b).

II. DERIVATION OF CENTRAL RESULT

Consider a classical system described by a Hamiltonian $H(\Gamma; \lambda)$, where $\Gamma = (\mathbf{q}, \mathbf{p})$ denotes a point in the system's phase space (a *microstate*), and λ is an externally controlled parameter, such as the piston location in the above

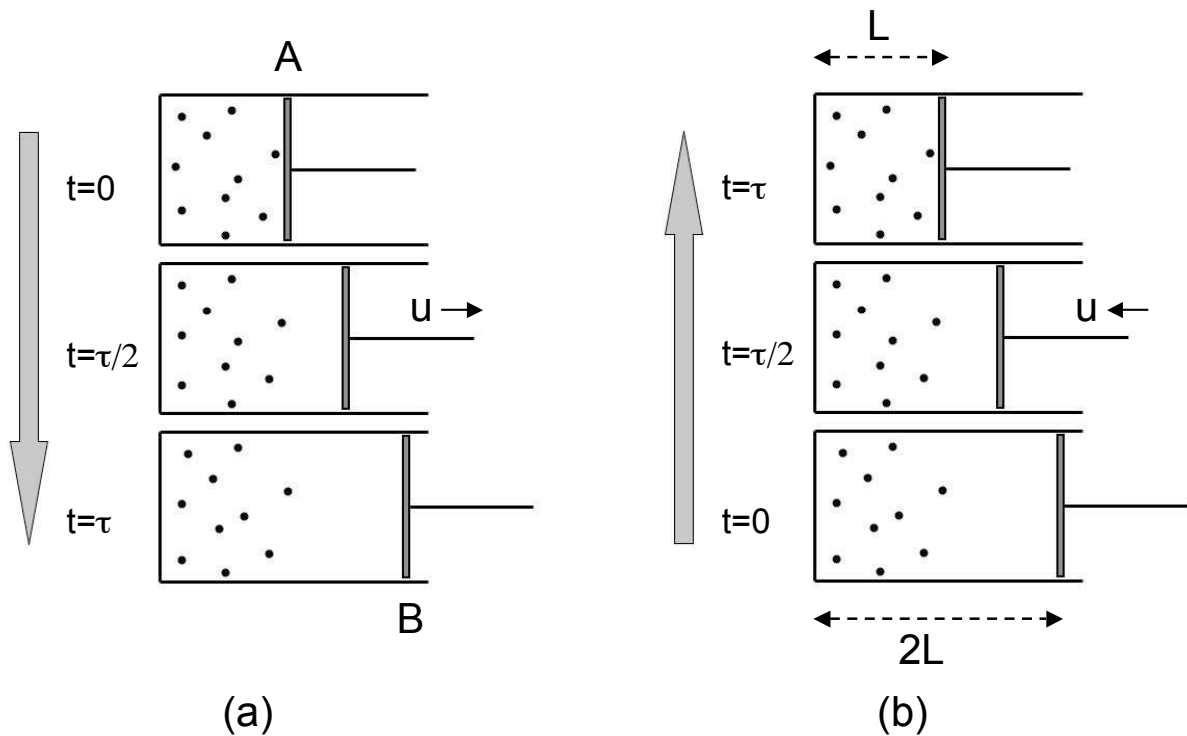


FIG. 3: (a) A typical realization of the forward process. Due to the great speed of the piston (Eq. 10), most particles remain in the left half the box for the duration of the process. (b) The conjugate twin of the realization depicted in (a). Almost all particles begin in the left half of the box, and the piston then moves rapidly through a largely empty region. (The vertical gray arrows specify the direction of increasing time.)

example. For every value of λ , assume H is time-reversal invariant:

$$H(\Gamma^*; \lambda) = H(\Gamma; \lambda) \quad , \quad \Gamma^* \equiv (\mathbf{q}, -\mathbf{p}). \quad (13)$$

This system can be prepared in an equilibrium state, by placing it in weak thermal contact with a sufficiently large heat reservoir at temperature T , holding the parameter fixed at a value λ , and then removing the reservoir after a sufficiently long relaxation time. This generates a microstate Γ_0 that is a random sample from the Boltzmann-Gibbs distribution,

$$p_\lambda(\Gamma_0) = \frac{1}{Z_\lambda} \exp[-\beta H(\Gamma_0; \lambda)], \quad (14)$$

where $Z_\lambda = \int d\Gamma \exp[-\beta H(\Gamma; \lambda)]$ is the partition function. The free energy associated with this equilibrium state is

$$F_\lambda = -\beta^{-1} \ln Z_\lambda. \quad (15)$$

In the analysis and discussions below, the dependence of p_λ , Z_λ , and F_λ on temperature will be left implicit, and equilibrium states will be identified by the parameter value λ .

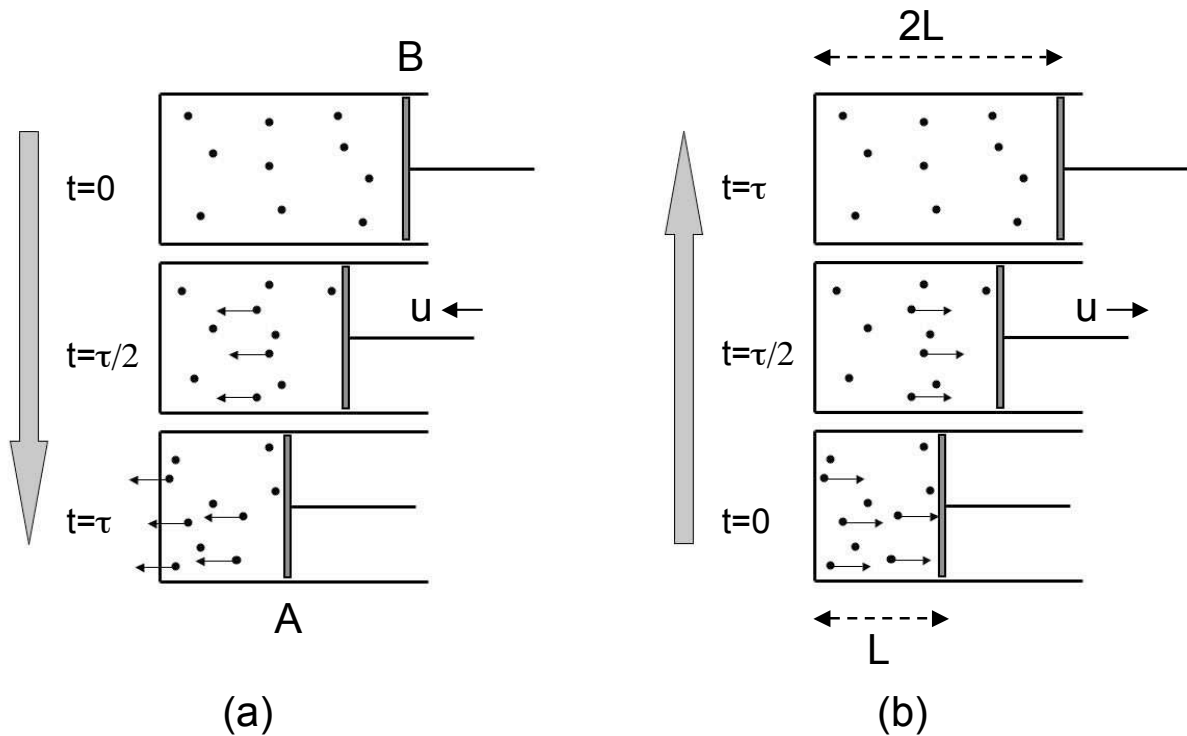


FIG. 4: (a) A typical realization of the reverse process. As the piston moves rapidly into the gas, the particles with which it collides gain large components of velocity ($\sim 2u$) along the direction of motion of the piston. The particles with the attached arrows are meant to represent these fast particles, while the unadorned ones are characterized by thermal velocities. (b) The conjugate twin of the realization depicted in (a). Half the particles are initially moving at great speeds ($\sim 2u$) in the direction of the piston. By the end of the process, after each of these has collided with the piston, the velocity distribution of the entire gas is thermal.

To perform the forward process (F), we first prepare the system in the equilibrium state A , then we remove the heat reservoir. Then, from $t = 0$ to $t = \tau$ we let the system evolve under Hamilton's equations as we vary λ from A to B according to a pre-determined schedule, λ_t^F . Let $H_t^F(\Gamma) = H(\Gamma; \lambda_t^F)$ denote the time-dependent Hamiltonian obtained when λ is varied in this manner, and let $\gamma^F = [\Gamma_t^F]_0^\tau$ denote a phase space trajectory evolving under this Hamiltonian. The notation indicates that the trajectory γ^F passes through the set of points Γ_t^F , for $0 \leq t \leq \tau$. Such a trajectory describes the microscopic history of the system during a single realization of the forward process.

By repeating this process infinitely many times, we generate a sequence of trajectories, $\{\gamma_1^F, \gamma_2^F, \dots\}$. These can be viewed as random samples from a probability distribution $\mathcal{P}^F[\gamma^F]$, defined on the set of all possible trajectories generated by H_t^F . Because the dynamics are deterministic, the probability of observing a given trajectory is simply that of sampling its initial conditions from a canonical distribution [6]:

$$\mathcal{P}^F[\gamma^F] = p_A(\Gamma_0^F) = \frac{1}{Z_A} \exp[-\beta H(\Gamma_0^F; A)]. \quad (16)$$

Since the system is thermally isolated (not in contact with a heat reservoir) as λ is varied from A to B , the work

performed on the system is equal to the net change in its energy:

$$W^F[\gamma^F] = H(\Gamma_\tau^F; B) - H(\Gamma_0^F; A). \quad (17)$$

Similar remarks and notation apply to the reverse process (R). The system is prepared in equilibrium state B , then λ is varied from B to A (Eq. 6), generating a Hamiltonian trajectory $\gamma^R = [\Gamma_t^R]_0^\tau$, with probability

$$\mathcal{P}^R[\gamma^R] = p_B(\Gamma_0^R) = \frac{1}{Z_B} \exp[-\beta H(\Gamma_0^R; B)]. \quad (18)$$

The work performed is

$$W^R[\gamma^R] = H(\Gamma_\tau^R; A) - H(\Gamma_0^R; B). \quad (19)$$

As mentioned in Section I, every forward trajectory γ^F has a conjugate twin γ^R (Fig. 2), that is a solution of Hamilton's equations when the parameter is varied according to the reverse schedule. In the remainder of this paper, whenever γ^F and γ^R appear together (e.g. in the same equation or sentence) it will be understood that these two trajectories form such a conjugate pair.

From Eqs.13, 17 and 19, we get

$$W^F[\gamma^F] = -W^R[\gamma^R] \quad ; \quad (20)$$

the work during a forward realization is the opposite of that during its conjugate twin. In what follows it will be convenient to deal with *dissipated* work values

$$W_d^F[\gamma^F] \equiv W^F[\gamma^F] - \Delta F \quad (21a)$$

$$W_d^R[\gamma^R] \equiv W^R[\gamma^R] + \Delta F = -W_d^F[\gamma^F]. \quad (21b)$$

(The term ‘‘dissipated work’’ here means the amount by which the work W exceeds that which would have been performed, had the process been carried out reversibly *and isothermally*.) In terms of these quantities, Eq. 7 becomes

$$\left\langle e^{-\beta W_d} \right\rangle_F = 1 \quad , \quad \left\langle e^{-\beta W_d} \right\rangle_R = 1. \quad (22)$$

We now have the elements in place to investigate the nature of those realizations that dominate the average $\langle e^{-\beta W} \rangle_F$, or, equivalently, $\langle e^{-\beta W_d} \rangle_F$. Combining Eqs.8, 13, 15-18, we obtain a simple relationship between the probability of observing a trajectory γ^F during the forward process, and that of observing its twin γ^R during the reverse:

$$\frac{\mathcal{P}^F[\gamma^F]}{\mathcal{P}^R[\gamma^R]} = \exp\left(\beta W_d^F[\gamma^F]\right) = \exp\left(-\beta W_d^R[\gamma^R]\right). \quad (23)$$

This result, originally obtained by Crooks for stochastic, Markovian dynamics [2], has here been derived in the context of Hamiltonian evolution.

(In Eqs.16 and 18, as in Ref. [6], the Liouville measure on initial conditions in phase space has implicitly been used to define a measure on the space of trajectories: the ‘‘volume’’ of trajectory space, $d\gamma^F$, associated with a collection of forward trajectories, is taken to be the phase space volume $d\Gamma_0^F$ occupied by their initial conditions. Liouville's theorem then implies that the volume occupied by a given set of forward trajectories is equal to that of the conjugate set of reverse trajectories. In this sense, the numerator and denominator in Eq.23 are defined with respect to the same measure on trajectory space.)

Let us now write $\langle e^{-\beta W_d} \rangle_F$ as an integral over forward trajectories:

$$1 = \left\langle e^{-\beta W_d} \right\rangle_F = \int d\gamma^F \mathcal{P}^F[\gamma^F] e^{-\beta W_d^F[\gamma^F]} \equiv \int d\gamma^F \mathcal{Q}^F[\gamma^F], \quad (24)$$

where $\mathcal{Q}^F = \mathcal{P}^F e^{-\beta W_d^F}$. Let ζ_{typ}^F and ζ_{dom}^F denote the regions of trajectory space where \mathcal{P}^F and \mathcal{Q}^F , respectively, are peaked, as illustrated in Fig.5. Thus, while ζ_{typ}^F contains the *typical* forward realizations, ζ_{dom}^F contains the *dominant* ones, since the greatest contribution in Eq.24 comes from the peak region of \mathcal{Q}^F .

For the reverse process, we have

$$1 = \left\langle e^{-\beta W_d} \right\rangle_R = \int d\gamma^R \mathcal{P}^R[\gamma^R] e^{-\beta W_d^R[\gamma^R]} \equiv \int d\gamma^R \mathcal{Q}^R[\gamma^R], \quad (25)$$

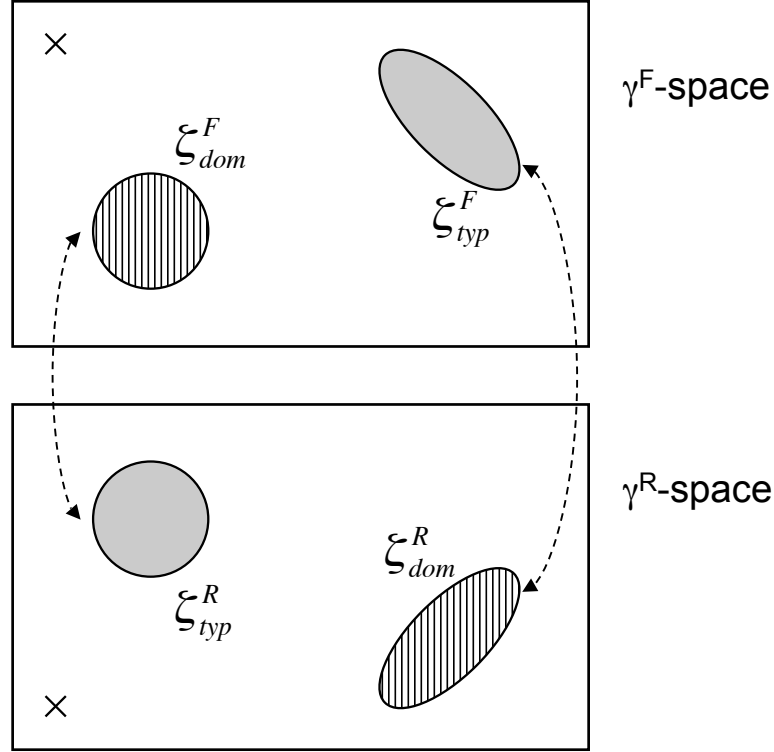


FIG. 5: The upper box represents the space of all forward trajectories, the lower box the space of reverse trajectories, and in this visual depiction conjugate pairing is indicated by reflection about a horizontal line between the two boxes (e.g. the two crosses represent a pair of conjugate twins). The grey regions ζ_{typ}^F and ζ_{typ}^R denote the peaks of the probability distributions \mathcal{P}^F and \mathcal{P}^R , while the vertically striped regions ζ_{dom}^F and ζ_{dom}^R are the peaks of the functions Q^F and Q^R . The dashed arrows indicate the conjugate pairing that is the central result of this paper (Eq. 27).

and we define regions ζ_{typ}^R and ζ_{dom}^R where \mathcal{P}^R and Q^R are peaked.

Combining Eq.23 with the definitions of Q^F and Q^R , we get

$$Q^F[\gamma^F] = \mathcal{P}^R[\gamma^R] \quad (26a)$$

$$Q^R[\gamma^R] = \mathcal{P}^F[\gamma^F]. \quad (26b)$$

Eq. 26a states that the function Q^F is the conjugate image of the distribution \mathcal{P}^R ; thus if we plot \mathcal{P}^R in the lower box of Fig. 5, then its mirror image in the upper box is Q^F . It follows that the trajectories in ζ_{dom}^F (the peak region of Q^F) are the conjugate twins of those in ζ_{typ}^R (the peak region of \mathcal{P}^R):

$$\zeta_{dom}^F \leftrightarrow \zeta_{typ}^R, \quad (27a)$$

where the symbol \leftrightarrow indicates a correspondence through conjugate pairing of trajectories. This is illustrated by the pair of circles in Fig. 5, depicting the peak regions of Q^F and \mathcal{P}^R . Similarly, Eq. 26b gives us

$$\zeta_{dom}^R \leftrightarrow \zeta_{typ}^F, \quad (27b)$$

as illustrated by the ellipses in Fig. 5. Thus the trajectories typically observed during the reverse process are the conjugate twins of those that dominate $\langle e^{-\beta W} \rangle$ for the forward process (Eq.27a), and vice-versa (Eq.27b). This is the central result of this paper.

Let us consider for a moment the special case of a *cyclic* process, for which the final value of the work parameter is the same as the initial value: $\lambda_0^F = A = B = \lambda_\tau^F$. In this situation $\Delta F = 0$, identically, and Eq. 1 becomes

$$\left\langle e^{-\beta W} \right\rangle_F = 1, \quad (28)$$

a result originally derived by Bochkov and Kuzovlev [31]. Under the additional assumption of a time-symmetric schedule, $\lambda_t^F = \lambda_{\tau-t}^F$, the forward and reverse processes are identical. Thus, for processes that are time-symmetric (and therefore also cyclic), there is no distinction between “forward” and “reverse”, and Eq. 27 is particularly easy to state: the exponential average is dominated by the conjugate twins of typical realizations.

In the analysis leading to Eq. 27, it has implicitly been assumed that the distributions $\mathcal{P}^F[\gamma^F]$ and $\mathcal{P}^R[\gamma^R]$ are sharply peaked, i.e. that each process is characterized by well-defined “typical behavior”. This assumption is often reasonable for systems with many degrees of freedom (see e.g. Figs. 3a, 4a). It is useful, however, to formalize and generalize the discussion, so as to avoid reliance on the notion of typicality.

Let S^F denote an arbitrary set of forward trajectories, and define

$$\Omega^F\{S^F\} \equiv \int_{S^F} d\gamma^F \mathcal{P}^F[\gamma^F] \quad , \quad \Psi^F\{S^F\} \equiv \int_{S^F} d\gamma^F \mathcal{Q}^F[\gamma^F]. \quad (29)$$

Ω^F is the probability of obtaining a trajectory in S^F , when carrying out the forward process; I will refer to this as the *statistical weight* of the set S^F in the ensemble of forward trajectories. In turn, Ψ^F provides a measure of the *relative contribution* of S^F to the average $\langle e^{-\beta W} \rangle_F$ (see Eq. 24). Note that $\Omega^F = \Psi^F = 1$ when S^F includes all forward trajectories. Define analogous quantities Ω^R and Ψ^R for a set of reverse trajectories S^R . Now take these two sets to be related by conjugate pairing: S^F is an arbitrary region in the upper box of Fig. 5, and S^R is its mirror image in the lower box. Using Eq.26 we then get

$$\Psi^F\{S^F\} = \Omega^R\{S^R\}. \quad (30)$$

In words: the relative contribution of a set of forward trajectories to $\langle e^{-\beta W} \rangle_F$, is equal to the statistical weight of the conjugate set of reverse trajectories. Of course, the converse is true as well: $\Psi^R\{S^R\} = \Omega^F\{S^F\}$.

Eq. 27 is a special case of Eq.30: if ζ_{typ}^R contains 95% of the statistical weight of all reverse trajectories (a reasonable definition of the peak region of \mathcal{P}^R), then the conjugate set of forward trajectories provides 95% of the contribution to $\langle e^{-\beta W} \rangle_F$.

As an illustration of Eq. 30 using the piston-and-gas example, consider the set S_n^F of all forward realization for which there are exactly n piston-particle collisions, and the conjugate set S_n^R of reverse trajectories. Then

$$\Psi^F\{S_n^F\} = \Omega^R\{S_n^R\}, \quad (31)$$

i.e. the relative contribution of n -collision realizations to $\langle e^{-\beta W} \rangle_F$, is exactly the probability of observing n collisions when performing the reverse process, for any $n \geq 0$. Since $\Omega^R\{S_n^R\}$ is peaked around $n \approx n_p/2$ (during compression we almost always observe roughly $n_p/2$ collisions, Fig. 4a), it follows that the greatest contribution to $\langle e^{-\beta W} \rangle_F$ comes from realizations of the expansion process for which $n \approx n_p/2$ (Fig. 4b).

III. NUMBER OF REALIZATIONS NEEDED FOR CONVERGENCE

When using Eq.2 to evaluate ΔF , how many realizations do we need to obtain a reasonable estimate? While a precise answer depends on the desired accuracy, a back-of-the-envelope estimate can be derived as follows.

Imagine that we repeatedly carry out the forward process, either in a laboratory experiment or using numerical simulations. In doing so we generate trajectories $\{\gamma_1^F, \gamma_2^F, \dots\}$ sampled from $\mathcal{P}^F[\gamma^F]$. Since the most important contribution to $\langle e^{-\beta W} \rangle_F$ comes from the region ζ_{dom}^F , we must sample this region to get a decent estimate of the average. The probability that a single randomly sampled trajectory falls within ζ_{dom}^F is

$$P = \int_{\zeta_{\text{dom}}^F} d\gamma^F \mathcal{P}^F[\gamma^F] = \int_{\zeta_{\text{typ}}^R} d\gamma^R \mathcal{P}^R[\gamma^R] \exp(-\beta W_d^R[\gamma^R]) \quad (32)$$

$$\sim \exp(-\beta \overline{W}_d^R) \int_{\zeta_{\text{typ}}^R} d\gamma^R \mathcal{P}^R[\gamma^R] \sim \exp(-\beta \overline{W}_d^R). \quad (33)$$

Here \overline{W}_d^R is the average work dissipated when performing the reverse process. On the first line we have used Eqs.23 and 27a, and on the second we have used the fact that the trajectories $\gamma^R \in \zeta_{\text{typ}}^R$ constitute most of the probability distribution \mathcal{P}^R . Thus an estimate of the number of realizations needed to obtain a single trajectory in ζ_{dom}^F is:

$$N_c^F = P^{-1} \sim \exp(\beta \overline{W}_d^R). \quad (34a)$$

The same argument gives us the expected number of reverse realizations needed to obtain a trajectory in ζ_{dom}^R :

$$N_c^R \sim \exp(\beta \overline{W}_d^F). \quad (34b)$$

These results suggest that the number of realizations required for convergence grows exponentially in the average dissipated work, in agreement with the findings of Gore *et al.* [32], and therefore exponentially with system size (assuming dissipated work is an extensive property), as concluded by Lua and Grosberg [27]. Interestingly, however, it is the average amount of work dissipated during the *reverse* process that determines the convergence of $\langle e^{-\beta W} \rangle$ for the *forward* process (Eq.34a), and vice-versa (Eq.34b). This implies that, of the two processes, the more dissipative one is the one for which $\langle e^{-\beta W} \rangle$ converges more rapidly. We can understand this counterintuitive conclusion with the following plausibility argument. Fig. 6 depicts the work distributions $\rho^F(W)$ and $\rho^R(-W)$, when $\overline{W}_d^F > \overline{W}_d^R$: the mean of ρ^F is displaced farther to the right of ΔF than the mean of ρ^R is to the left of ΔF , which in turn suggests that ρ^F is wider than ρ^R , since the two distributions cross exactly at $W = \Delta F$ [20]. Thus, as measured in standard deviations, we must reach deeper into the tail of ρ^R to sample the peak region of ρ^F , than the other way around. Hence $N_c^R > N_c^F$ when $\overline{W}_d^F > \overline{W}_d^R$. This prediction agrees well with recent numerical simulations of an asymmetric object dragged through a hard-disk gas [33].

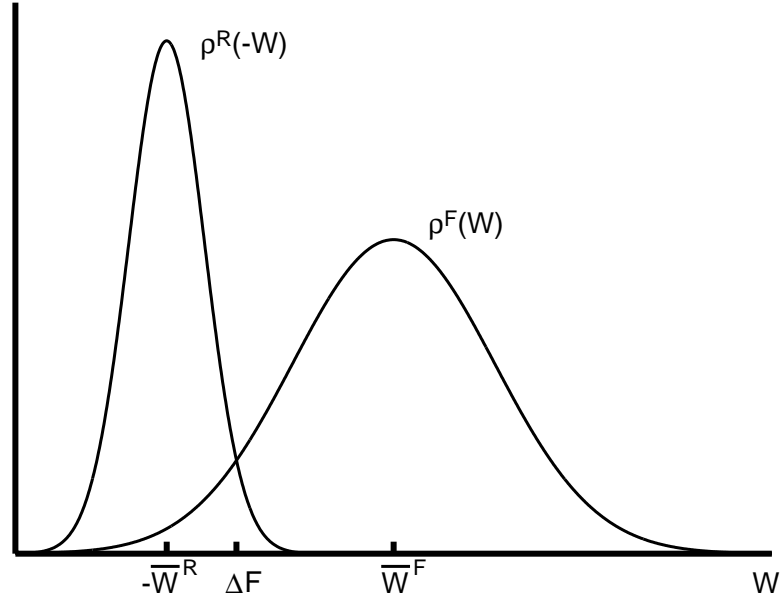


FIG. 6: Distributions of work values when $\overline{W}_d^F > \overline{W}_d^R$. Since the two distributions cross at $W = \Delta F$, ρ^F is wider than ρ^R . Thus, work values near $-\overline{W}^R$ are more frequently sampled from $\rho^F(W)$, than those near \overline{W}^F are sampled from $\rho^R(-W)$.

The piston-and-gas example provides a nice illustration of Eq. 34. From Section I we have $\overline{W}^F \approx 0$, $\overline{W}^R \approx n_p m u^2$, and $\Delta F = -n_p \beta^{-1} \ln 2$, thus

$$\overline{W}_d^F \approx n_p \beta^{-1} \ln 2 \quad , \quad \overline{W}_d^R \approx n_p (m u^2 - \beta^{-1} \ln 2). \quad (35)$$

Hence $\overline{W}_d^R \gg \overline{W}_d^F$ in the fast piston limit (Eq. 10); rapid compression is much more dissipative than rapid expansion.

Let us now analyze the convergence of $\langle e^{-\beta W} \rangle_R$. The dominant realizations are those for which essentially all the gas particles begin in the left half of the box (Fig.3b). The probability of generating such an initial condition is

$(1/2)^{n_p}$, hence the number of realizations needed to observe a single such event is

$$N_c^R \sim 2^{n_p}, \quad (36)$$

which is equal to $\exp(\beta \overline{W}_d^F)$, as predicted by Eq.34b.

For the convergence of $\langle e^{-\beta W} \rangle_F$, the dominant realizations are represented by Fig.4b: initially, half the particles are characterized by a thermal velocity profile, the other half with $v_x \approx 2u$. The probability of generating such a microstate is roughly

$$\frac{n_p!}{(n_p/2)!(n_p/2)!} \cdot a^{n_p/2}. \quad (37)$$

The first factor counts the number of ways of choosing which $n_p/2$ particles start with $v_x \approx 2u$, and $a \equiv \exp[-\beta m(2u)^2/2]$ is an estimate of the probability for a single particle to have a such a large initial v_x . Using Stirling's approximation for the factorials, Eq.37 reduces to $2^{n_p} \cdot \exp(-n_p \beta m u^2)$. Taking the reciprocal, we get

$$N_c^F \sim \exp[n_p(\beta m u^2 - \ln 2)], \quad (38)$$

which is equal to $\exp(\beta \overline{W}_d^R)$, as predicted by Eq.34a. Since the fast piston limit (Eq. 10) implies $\beta m u^2 \gg 1$, it is legitimate to drop the $\ln 2$ term in this result, obtaining $N_c^F \sim \exp(n_p \beta m u^2)$. This is consistent with the calculations of Lua and Grosberg, who obtain $N_c^F \sim \exp(\beta m L^2/\tau^2)$ when $n_p = 1$ (see section 4 of Ref. [27]).

These results verify that the more dissipative process (compression) is the one for which the exponential average converges more rapidly. We can understand why this is the case, without performing explicit quantitative estimates. For the compression process, as mentioned, a dominant realization begins with all the particles in the left half of the box, thus n_p particles must simultaneously satisfy a condition that is not so unusual for any given particle. For the expansion process, on the other hand, half the particles must begin with $v_x \approx 2u$, therefore $n_p/2$ particles must simultaneously satisfy a condition that is very unusual for even a single particle (since $u \gg v_{\text{th}}$). The latter situation is the less likely by far. Of course, when $n_p \gg 1$, both N_c^F and N_c^R are extremely large [34].

In practice, the convergence difficulties associated with Eq. 1 are mitigated somewhat if we have data for both the forward and the reverse processes. In that case, Bennett's *acceptance ratio method* [20, 35, 36, 37] converges faster than a direct exponential average of either the forward or reverse work values. It would be useful to derive a simple estimate, analogous to Eq. 34, of the number of realizations required for this method to converge, and to develop heuristic insight regarding the realizations that make the most important contribution to the acceptance ratio estimate of ΔF .

Finally, recall that a measure of the difference between two normalized distributions, f_1 and f_0 , is given by the *relative entropy* [38]

$$D[f_1|f_0] = \int f_1 \ln \frac{f_1}{f_0} \geq 0, \quad (39)$$

where the integral is over the space of variables on which f_0 and f_1 are defined. Applying this definition to the forward and reverse distributions of trajectories, and identifying γ^F with its twin γ^R , we get

$$D[\mathcal{P}^F|\mathcal{P}^R] = \int d\gamma^F \mathcal{P}^F[\gamma^F] \ln \frac{\mathcal{P}^F[\gamma^F]}{\mathcal{P}^R[\gamma^R]} = \beta \overline{W}_d^F, \quad (40a)$$

using Eq.23, and similarly

$$D[\mathcal{P}^R|\mathcal{P}^F] = \beta \overline{W}_d^R. \quad (40b)$$

Analogous identities have been derived for the steady states of Markov chains [39], and for the work distributions arising in the context of free energy estimation [40]; and the physical significance of relative entropy for equilibrium and nonequilibrium fluctuations has recently been discussed in Ref. [41]. Eq. 40 suggests that there might be a natural information-theoretic interpretation of Eq. 34.

IV. FREE ENERGY PERTURBATION

The *perturbation method* for estimating free energy differences is based on the identity

$$\left\langle e^{-\beta \Delta H} \right\rangle_A = e^{-\beta \Delta F}, \quad (41)$$

where $\Delta H(\Gamma) \equiv H(\Gamma; B) - H(\Gamma; A)$, and $\langle \cdots \rangle_A$ denotes an average over microstates Γ sampled from the canonical ensemble A [12, 42]. [In this section, I explicitly assume that the Hamiltonians $H(A)$ and $H(B)$ are finite-valued throughout phase space. This precludes situations such as the piston-and-gas example, particles with perfectly hard cores, etc.] The convergence problems that arise with the nonequilibrium work theorem also plague the free energy perturbation identity [43]. In the case of Eq.41, we can frame this issue by considering the *typical* microstates sampled from the equilibrium ensemble A , and the rare but *dominant* microstates that contribute most to the average of $e^{-\beta\Delta H}$. In what follows I discuss how the ideas developed in earlier sections of this paper apply to Eq. 41.

The left side of Eq. 41 is most naturally viewed as an equilibrium average, as described above. An alternative perspective, however, treats Eq. 41 as a special case of Eq. 1, obtained in the “instantaneous switching” limit, $\tau \rightarrow 0$, in which λ is changed suddenly from A to B [1]. The system then has no opportunity to evolve during the process, hence a realization is described not by a trajectory, but rather by a single microstate (sampled from A). The work W is given by ΔH , evaluated at this microstate. If we view Eq.41 as pertaining to a forward perturbation ($A \rightarrow B$), then the reverse perturbation involves sampling from equilibrium state B :

$$\left\langle e^{+\beta\Delta H} \right\rangle_B = e^{+\beta\Delta F}, \quad (42)$$

where ΔH and ΔF are defined identically in Eqs.41 and 42.

By analogy with Eq.24 we can rewrite Eq.41 as follows:

$$1 = \left\langle e^{-\beta W_d^A} \right\rangle_A = \int d\Gamma p_A(\Gamma) e^{-\beta W_d^A(\Gamma)} \equiv \int d\Gamma q_A(\Gamma), \quad (43)$$

where p_A is the equilibrium distribution for state A (Eq.14), and $W_d^A \equiv \Delta H - \Delta F$. Similarly rewriting Eq.42 (with $W_d^B \equiv -\Delta H + \Delta F$), let us now define ξ_{typ}^A , ξ_{dom}^A , ξ_{typ}^B , and ξ_{dom}^B as the regions of phase space where p_A , q_A , p_B , and q_B , respectively, are peaked. These contain the typical and dominant microstates for the two perturbations. Eq. 27 now becomes

$$\xi_{\text{dom}}^A = \xi_{\text{typ}}^B \quad , \quad \xi_{\text{dom}}^B = \xi_{\text{typ}}^A. \quad (44)$$

Thus, when implementing the free energy perturbation method, by sampling from one distribution (say, A), the collection of sampled microstates must be large enough to include a reasonable number that are typical of the other distribution (B), otherwise we will not achieve convergence of the exponential average. If there is very little overlap between the two equilibrium distributions in phase space, then the number of samples required to satisfy this condition is prohibitively large [12].

Lower bounds N_c^A and N_c^B on the required numbers of realizations are given by analogues of Eq. 34:

$$\ln N_c^A \sim \beta \overline{W}_d^B = D[p_B|p_A] \geq 0 \quad (45a)$$

$$\ln N_c^B \sim \beta \overline{W}_d^A = D[p_A|p_B] \geq 0, \quad (45b)$$

where the overbars now denote canonical averages with respect to the ensembles A and B . Of the two perturbations, the one with larger \overline{W}_d requires fewer samples for convergence of the exponential average.

These results are illustrated by Widom’s particle insertion method for computing a chemical potential [12, 44]. Imagine a fluid of $N + 1$ particles, and suppose that $H(A)$ describes the situation in which N of the particles interact with one another through a pairwise potential, while the remaining, “tagged” particle is uncoupled from the rest; and $H(B)$ describes the situation in which all $N + 1$ particles are mutually coupled via the pairwise potential. The free energy difference $\Delta F = F_B - F_A$ is the excess chemical potential of the fluid, provided N is large enough to recover bulk properties. In principle, we can estimate ΔF either by using the forward perturbation, $A \rightarrow B$ (particle insertion), or with the reverse perturbation, $B \rightarrow A$ (deletion).

In a dense fluid, particle insertion usually generates a very large value of ΔH , while for deletion ΔH is typically modest. Thus $\overline{W}_d^A > \overline{W}_d^B$, and Eq.45 predicts that the insertion method converges more rapidly than the deletion method, as indeed observed empirically [12]. To understand this in terms of typical and dominant microstates, note that when sampling from ensemble B , the (interacting) tagged particle typically occupies its own small volume within the fluid, from which the remaining particles are excluded. Thus, by Eq. 44, to achieve convergence in Eq.41 we must sample sufficiently from ensemble A to obtain microstates in which the *non-interacting*, tagged particle happens to sit inside a cavity created by the spontaneous fluctuations of the remaining N -particle fluid. This condition carries an entropic cost roughly equal to the free energy of forming a suitably large cavity.

Conversely, when sampling from ensemble A the (non-interacting) tagged particle is typically found within the repulsive core of one of the other particles, hence to succeed with the particle *deletion* method, we must generate such

microstates when sampling from ensemble B . This carries an enthalpic (energetic) cost, determined by the strength of the repulsive core of the pairwise potential. Because the repulsive cores are generally described by very steep potentials, this enthalpic penalty is much larger than the entropic penalty described above: thermal fluctuations are much more likely to generate a cavity large enough to accommodate a new particle, than they are to squeeze two particles into a volume meant only for one. Hence the dominant realizations of the forward perturbation (insertion), are much less rare than those of the reverse perturbation (deletion).

V. DISCUSSION

The central result of this paper, Eq. 27, is a duality that relates the dominant realizations of a given process to typical realizations of the conjugate process. In a nutshell, it states that to achieve convergence in Eq. 1 we must observe realizations during which the system appears as though it is evolving backward in time. I will now sketch an interpretation of this result similar to the discussion of *causal* and *anti-causal* response theory found in Ref. [45]. Following that, I will briefly discuss the validity of Eq. 27 in situations involving non-Hamiltonian (including stochastic) equations of motion.

Let us picture the ensemble of forward trajectories, $\{\gamma_1^F, \gamma_2^F, \dots\}$, as a swarm of points evolving independently in phase space (from $t = 0$ to $t = \tau$), and let $p^F(\Gamma, t) = \langle \delta(\Gamma - \Gamma_t^F) \rangle$ denote the corresponding time-dependent phase space distribution. This distribution obeys the Liouville equation,

$$\frac{\partial p^F}{\partial t} = \frac{\partial H_t^F}{\partial \mathbf{q}} \cdot \frac{\partial p^F}{\partial \mathbf{p}} - \frac{\partial H_t^F}{\partial \mathbf{p}} \cdot \frac{\partial p^F}{\partial \mathbf{q}}, \quad (46)$$

where $H_t^F = H(\Gamma; \lambda_t^F)$. The assumption of initial equilibrium is a boundary condition imposed at $t = 0$:

$$p^F(\Gamma, 0) = \frac{1}{Z_A} \exp[-\beta H(\Gamma; A)]. \quad (47)$$

Now consider a distribution $q^F(\Gamma, t)$ evolving under the same dynamics, Eq.46, but satisfying a boundary condition at $t = \tau$ (rather than at $t = 0$):

$$q^F(\Gamma, \tau) = \frac{1}{Z_B} \exp[-\beta H(\Gamma; B)]. \quad (48)$$

This distribution describes an ensemble that ends, rather than begins, in a state of thermal equilibrium. In the language of Ref. [45], p^F corresponds to a *causal* ensemble of trajectories, determined by initial conditions, while q^F is *anti-causal*, determined by final conditions. The central result of this paper can now be restated as follows: while the typical *causal* trajectories are the ones we ordinarily observe, the typical *anti-causal* trajectories are the ones that dominate the exponential average. This follows from the simple observation that the anti-causal ensemble of forward trajectories is just the conjugate image of the causal ensemble of reverse trajectories.

In the context of linear response theory, Evans and Searles [45] have shown that anti-causal ensembles give rise to Green-Kubo “anti-transport” coefficients. In an earlier theoretical study of dilute gases, Cohen and Berlin [46] derived an anti-causal version of the Boltzmann equation, by applying the assumption of molecular chaos to *future* rather than *past* pair distribution functions. In both papers the anti-causal behavior is associated with violations of the second law of thermodynamics: the Green-Kubo coefficients of Ref. [45] have the “wrong” signs, and the Boltzmann-like equation of Ref. [46] obeys an anti- H theorem. The situation is similar here: anti-causal ensembles are associated with negative average values of dissipated work; the second law of thermodynamics, by contrast, asserts that irreversible processes are accompanied by positive average dissipated work.

Eq. 23 provides an amusing connection between the conjugate pairing of trajectories (microscopic reversibility) and the second law of thermodynamics (macroscopic irreversibility), illustrated in the piston-and-gas context by the following thought experiment. Imagine that we are shown a movie in which we see the microscopic evolution of the gas as the piston moves outward from A to B , and we are asked to guess whether this movie depicts an actual realization of the expansion process, or whether, instead, a realization of the compression process was filmed, and now that movie is being run backward. I will refer to this as “guessing the direction of time”. To analyze this situation quantitatively, let γ^F specify the microscopic evolution we observe when watching this movie, and γ^R its conjugate twin. Then the task of guessing the direction of time is an exercise in statistical inference, in which we compare the likelihoods of two hypotheses. Specifically, we ask whether it is more likely that we obtain γ^F when performing the forward process, or γ^R when performing the reverse process. By Eq.23, the ratio of these likelihoods is $\exp(\beta W_d^F)$. Hence if $W_d^F > 0$, we opt for the first hypothesis, namely that the piston was indeed withdrawn from A to B ; whereas

if $W_d^F < 0$ (equivalently $W_d^R > 0$) then we guess that the piston was pushed into the gas, and we are seeing a movie of that process in time-reversed order. Thus when asked to guess the arrow of time, we optimize our answer simply by insisting that the sign of the dissipated work be positive, in agreement with the second law.

It is natural to use Hamilton's equations to describe a thermally isolated classical system, as in this paper. If the system is in contact with a heat reservoir, however, then there are various ways to model its evolution. The most intuitively natural is to treat the combined system *and reservoir* as a very large, Hamiltonian system. Alternatively, one can describe the evolution of the system itself using stochastic equations of motion, such as the Metropolis Monte Carlo algorithm, or Langevin dynamics. Yet another approach involves deterministic but non-Hamiltonian equations of motion, such as Gaussian thermostats, designed to mock up the presence of a heat reservoir. Eq.1 has been derived for all these cases, so it is natural to ask whether the central result of the present paper, Eq. 27, also holds for these various schemes.

Since the heart of the argument in Section II follows from Eq. 23, two conditions are sufficient for the central results of this paper to hold for any given one of the above-mentioned schemes. First, there must exist a conjugate pairing of forward and reverse trajectories. Second, the probability of observing a particular trajectory γ^F during the forward process, and that of observing its twin γ^R during the reverse process, must satisfy Eq. 23. These conditions have been verified explicitly when the system evolves under a discrete-time Monte Carlo scheme satisfying detailed balance (such as the Metropolis algorithm) [2] or under Langevin dynamics [47, 48, 49]. When the evolution of the system is modeled with isokinetic Gaussian equations of motion, the validity of Eq. 23 follows from the analysis of Ref. [7]. Thus Eq. 27 of the present paper applies when these schemes are used to model the evolution of the system.

When the system and reservoir are treated together as a very large, Hamiltonian system, then Eq. 23 can be derived by repeating the steps of Section II, but working in the *full* phase space containing all the interacting degrees of freedom, and then projecting out the reservoir degrees of freedom. The analysis becomes slightly complicated if the coupling between the system and reservoir is not negligible, but this technical issue is handled much as in Ref. [9] (see, however, Refs. [50, 51]), and the details will not be presented here.

Finally, the nonequilibrium work theorem is just one of a number of (mostly recent) predictions concerning the statistical mechanics of systems far from thermal equilibrium. Others include the Kawasaki identity [52] and its generalization by Morriss and Evans [53], the *fluctuation theorem* [54, 55, 56, 57, 58, 59, 60, 61], Hatano and Sasa's equality for transitions between nonequilibrium steady states [62, 63, 64], and Adib's microcanonical version of Eq. 1 [65]. It remains to be investigated whether the analysis of the present paper is valid (and relevant) in the context of these other, closely related results.

It is a pleasure to acknowledge useful correspondence with Alexander Grosberg and Rhonald Lua. This work was supported by the United States Department of Energy, under contract W-7405-ENG-36.

-
- [1] C. Jarzynski, Phys. Rev. Lett. **78**, 2690 (1997); Phys. Rev. E **56**, 5018 (1997).
 - [2] G.E.Crooks, J.Stat.Phys.**90**, 1481 (1998).
 - [3] G.E. Crooks, Phys. Rev. E **60**, 2721 (1999).
 - [4] G. Hummer and A. Szabo, Proc. Natl. Acad. Sci. (USA) **98**, 3658 (2001).
 - [5] R.M. Neal, Statistics and Computing **11**, 125 (2001).
 - [6] S.X. Sun, J. Chem. Phys. **118**, 5769 (2003)
 - [7] D.J. Evans, Mol. Phys. **101**, 1551 (2003).
 - [8] H. Oberhofer, C. Dellago, and P. Geissler, J. Phys. Chem. B **109**, 6902 (2005).
 - [9] C. Jarzynski, J. Stat. Mech.: Theor. Exp. P09005 (2004).
 - [10] A. Imparato and L. Peliti, Europhys. Lett. **69**, 643 (2005).
 - [11] C. Jarzynski, in *Lecture Notes in Physics* **597**, Springer Verlag, Berlin, 2002, eds. P.Garbaczewski and R.Olkiewicz.
 - [12] D. Frenkel and B. Smit, *Understanding Molecular Simulation: from Algorithms to Applications*, Chapter 7. Academic Press, San Diego, 2002.
 - [13] F. Ritort, Séminaire Poincaré **2**, 193 (2003).
 - [14] S. Park and K. Schulten, J. Chem. Phys. **120**, 5946 (2004).
 - [15] G. Hummer and A. Szabo, Acc. Chem. Res. **38**, 504 (2005).
 - [16] C. Bustamante, J. Liphardt, and F. Ritort, Physics Today **58**, 43 (2005).
 - [17] J. Liphardt, S. Dumont, S. Smith, I. Tinoco, and C. Bustamante, Science **296**, 1832 (2002).
 - [18] F. Douarache, S. Ciliberto, A. Petrosyan, and I. Rabbiosi, Europhys. Lett. **70**, 593 (2005).
 - [19] F. Douarache, S. Ciliberto, and A. Petrosyan, J. Stat. Mech.: Theor. Exp. P09011 (2005).
 - [20] D. Collin *et al.*, Nature **437**, 231 (2005).
 - [21] S. Yukawa, J. Phys. Soc. Japan **69**, 2367 (2000).
 - [22] J. Kurchan, cond-mat/0007360.

- [23] S. Mukamel, Phys. Rev. Lett. **90**, 170604 (2003).
- [24] W. De Roeck and C. Maes, Phys. Rev. E **69**, 026115 (2004).
- [25] T. Monnai, Phys. Rev. E **72**, 027102 (2005)
- [26] F. Ritort, J. Stat. Mech.: Theor. Exp. P10016 (2004).
- [27] R.C. Lua and A.Y. Grosberg, J. Phys. Chem. B **109**, 6805 (2005).
- [28] J. Sung, cond-mat/0506214.
- [29] R.C. Lua, cond-mat/0511302.
- [30] I. Bena, C. Van den Broeck, and R. Kawai, Europhys. Lett. **71**, 879 (2005).
- [31] G.N. Bochkov and Yu.E. Kuzovlev, Zh. Eksp. Teor. Fiz. **72**, 238 (1977) [Sov. Phys.–JETP **45**, 125 (1977)]; Physica **106A**, 443 (1981); Physica **106A**, 480 (1981).
- [32] J. Gore, F. Ritort, and C. Bustamante, Proc. Natl. Acad. Sci. (USA) **100**, 12564 (2003).
- [33] B. Cleuren, C. Van den Broeck, and R. Kawai, cond-mat/0511653.
- [34] D.H.E. Gross, cond-mat/0509648.
- [35] C.H. Bennett, J. Comp. Phys. **22**, 245 (1976).
- [36] G.E. Crooks, Phys. Rev. E **61**, 2361 (2000).
- [37] M.R. Shirts *et al.*, Phys. Rev. Lett. **91**, 140601 (2003).
- [38] T.M. Cover and J.A. Thomas, *Elements of Information Theory*, John Wiley and Sons, Inc., New York, 1991.
- [39] P. Gaspard, J. Stat. Phys. **117**, 599 (2004).
- [40] D. Wu and D.A. Kofke, J. Chem. Phys. **123**, 054103 (2005).
- [41] H. Qian, Phys. Rev. E **63**, 042103 (2001).
- [42] R. Zwanzig, J. Chem. Phys. **22**, 1420 (1954).
- [43] See e.g. D.M. Zuckerman and T.B. Woolf, J. Stat. Phys. **114**, 1303 (2004).
- [44] B. Widom, J. Chem. Phys. **39**, 2802 (1963).
- [45] D.J. Evans and D.J. Searles, Phys. Rev. E **53**, 5808 (1996).
- [46] E.G.D. Cohen and T.H. Berlin, Physica **26**, 717 (1960).
- [47] C. Jarzynski, Acta Phys. Pol. **29**, 1609 (1998).
- [48] J. Kurchan, cond-mat/0511073.
- [49] V. Chernyak, M. Chertkov, and C. Jarzynski, manuscript in preparation.
- [50] E.G.D. Cohen and D. Mauzerall, J. Stat. Mech.: Theor. Exp. P07006 (2004).
- [51] E.G.D. Cohen and D. Mauzerall, Mol. Phys. **103**, 2923 (2005).
- [52] T. Yamada and K. Kawasaki, Prog. Theor. Phys. **38**, 1031 (1967).
- [53] G.P. Morriss and D.J. Evans, Mol. Phys. **54**, 629 (1985).
- [54] D.J. Evans, E.G.D. Cohen, and G.P. Morriss, Phys. Rev. Lett. **71**, 2401 (1993).
- [55] D.J. Evans and D.J. Searles, Phys. Rev. E **50**, 1645 (1994).
- [56] G. Gallavotti and E.G.D. Cohen, J. Stat. Phys. **80**, 931 (1995).
- [57] J. Kurchan, J. Phys. A **31**, 3719 (1998).
- [58] J.L. Lebowitz and H. Spohn, J. Stat. Phys. **95**, 333 (1999).
- [59] C. Maes, J. Stat. Phys. **95**, 367 (1999).
- [60] D.J. Evans and D. Searles, Adv. Phys. **51**, 1529 (2002).
- [61] G.M. Wang *et al.*, Phys. Rev. Lett. **89**, 050601 (2002).
- [62] T. Hatano, Phys. Rev. E **60**, R5017 (1999).
- [63] T. Hatano, S.I. Sasa, Phys. Rev. Lett. **86**, 3463 (2001).
- [64] E. Trepagnier *et al.*, Proc. Natl. Acad. Sci. (USA) **101**, 15038 (2004).
- [65] A.B. Adib, Phys. Rev. E **71**, 056128 (2005).